Carbohydrate Polymers 112 (2014) 359–366

Contents lists available at ScienceDirect

Carbohydrate Polymers

journal homepage: www.elsevier.com/locate/carbpol

Ginsenoside compound K-bearing glycol chitosan conjugates: Synthesis, physicochemical characterization, and *in vitro* biological studies

Ramya Mathiyalagan [a], Sathiyamoorthy Subramaniyam [a,c], Yeon Ju Kim [a,*], Youn-Chul Kim [b], Deok Chun Yang [a,*]

[a] Graduate School of Biotechnology and Ginseng Bank, College of Life Sciences, Kyung Hee University, Yongin 446-701, Republic of Korea
[b] Standardized Material Bank for New Botanical Drugs, College of Pharmacy, Wonkwang University, Iksan 570-749, Republic of Korea
[c] Insilicogen Inc., #909, Venture Valley, 958, Gosaek-dong, Gwonseon-gu, Suwon, Gyeonggi-do 441-813, South Korea

ARTICLE INFO

Article history:
Received 17 March 2014
Received in revised form 21 May 2014
Accepted 29 May 2014
Available online 10 June 2014

Keywords:
Ginsenosides
Compound K
Glycol chitosan
Self-assembled nanoparticles
Tumor
Anti-cancer efficacy

ABSTRACT

Ginsenosides are triterpenoids found in *Panax ginseng* and have a numerous structural, functional, and pharmacological properties. The purpose of this study was to develop hydrophilic polymer functionalized ginsenoside conjugates to enhance water solubility and targeted delivery. To this end, hydrophobic ginsenoside compound K (CK) was covalently conjugated to the backbone of hydrophilic glycol chitosan (GC) through an acid-labile linkage. The resulting GC–CK conjugates formed self-assembled spherical nanoparticles in an aqueous solution, and their particles sizes were (296 nm and 255 nm) dependent on the degree of CK substitution. The nanoparticles were stable in the physiological buffer (pH 7.4) over a period of 8 days, whereas they were readily degraded under acidic conditions (pH 5.0) mimicking the intracellular pH-conditions. From *in vitro* release experiment, it was found that CK released slowly from the self-assembled nanoparticles in the physiological buffer (pH 7.4). On the other hand, the release rate of CK was rapidly increased under the acidic condition (pH 5.0). *In vitro* cytotoxicity assays revealed that GC–CK conjugates exhibited higher cytotoxicity than CK in HT29, and similar cytotoxicity in HepG2, and HT22 cell lines. Moreover, RAW264.7 cells treated with GC–CK maintained good cell viability and exhibited decreased lipopolysaccharide-induced NO production. Taken together, these results suggest that the GC–CK conjugate may be potentially useful as a tumor-specific delivery vehicle.

© 2014 Elsevier Ltd. All rights reserved.

1. Introduction

Cancer is a leading cause of death worldwide. Although numerous highly active pharmacological anticancer drugs are available, their distribution throughout body due to the lack of tumor-targeting, poor water-solubility, systemic toxicity, and short half-life in blood circulation are all major drawbacks that limit their use in cancer chemotherapy. Conjugation of anticancer drugs with water-soluble polymers has been proposed as a way to surmount these issues (Goodarzi, Varshochian, Kamalinia, Atyabi, & Dinarvand, 2013). Indeed, such polymer conjugated anticancer drugs exhibit several advantages such as enhanced water-solubility of hydrophobic drugs and prolonged circulation time of drugs in the bloodstream (Park et al., 2007), as well as reduced off-target cytotoxicity, protection of drugs against deactivation (Goodarzi et al., 2013), and increased accumulation in tumor tissues as a result of the enhanced permeation and retention (EPR) effect (Min et al., 2008). Numerous drug delivery carriers such as polymer–drug conjugates, micelles, nanoparticles, and stealth liposomes have been investigated for efficient drug delivery (Deepagan, Thambi, Ko, Kang, & Park, 2013; Lee, Koo, et al., 2011; Thambi, Deepagan, Yoo, & Park, 2011; Thambi, Yoon, et al., 2011; Thambi, Deepagan, Ko, Lee, & Park, 2012; Sivasubramanian, Thambi, & Park, 2013). In addition, cancer drugs encapsulated with nanosized drug carrier exhibit improved pharmacological efficacy compared with free drug (Duhem et al., 2012; Min et al., 2008; Thambi et al., 2014). Also, squalenoyl-based natural triterpene drug conjugates which could form self-assembled nanoparticles with improved antitumor activity of the anticancer drugs have been reported (Maksimenko, Alami, et al., 2014; Maksimenko, Dosio, et al., 2014).

Among the wide range of drug carriers, polysaccharides have been paid increasing attention as potent delivery vehicle due to their ideal physiochemical and biological properties (Felt, Buri,

* Corresponding authors. Tel.: +82 31 201 2100; fax: +82 31 205 2688.
E-mail addresses: ramyabinfo@gmail.com (R. Mathiyalagan), s.sathiyamurthi@gmail.com (S. Subramaniyam), yeonjukim@khu.ac.kr, yeonjukim0818@ymail.com (Y.J. Kim), yckim@wonkwang.ac.kr (Y.-C. Kim), dcyang@khu.ac.kr (D.C. Yang).

http://dx.doi.org/10.1016/j.carbpol.2014.05.098
0144-8617/© 2014 Elsevier Ltd. All rights reserved.

& Gurny, 1998). Among the polysaccharides being considered, chitosan has gained attention due to its excellent biodegradability, biocompatibility, as well as mucoadhesive interaction with the intestinal track and antibacterial, antifungal, and antioxidant properties (Jayakumar, Menon, Manzoor, Nair, & Tamura, 2010). Chitosan is a natural biopolymer composed of β-1, 4 linked N-acetyl-D-glucosamine and D-glucosamine, and is obtained by extensive deacetylation of chitin. Chitin is the second most abundant natural polysaccharide, and is found in vital component of crustaceans, shells of molluscs, cuticles of insects, and cell walls of fungi (Muzzarelli et al., 2012). Unfortunately, the use of organic acids to dissolve chitosan induces harmful effects, which is highly undesirable for drug delivery applications. As viable alternatives, gaseous CO_2 and alkaline NH_4HCO_3 were used to dissolve chitosan yielding thin films or gels (Gorczyca et al., 2014; Muzzarelli, Tosi, Francescangeli, & Muzzarelli, 2003).

In addition to improve the water solubility, hydrophilic chitosan derivatives such as glycol chitosan (GC) and carboxymethyl chitosan have also been developed. Owing to the biocompatibility and good water-solubility over a range of pH levels, GC has been extensively studied as a hydrophilic carrier for a variety of drugs and proteins (Park et al., 2006).

Similar to chitosan, GC conjugates has low toxicity, good biocompatibility, and exhibits improved uptake through endocytosis pathways (Nam et al., 2009). In addition, recent studies indicate that GC may be a biocompatible and versatile carrier for efficient delivery of therapeutic agents (Min et al., 2008; Quiñones et al., 2012, 2013; Yu, Li, Qiu, & Jin, 2008) and oral delivery of poorly soluble drugs (Duhem et al., 2012). Direct conjugation of anticancer drugs into hydrophilic polymers have various advantages over polymeric nanoparticles carriers such as increased drug half-life in the body and enhanced antitumor effects (Lee, Koo, et al., 2011).

Ginsenosides are triterpene saponins and are the main active component in Korean Ginseng (*Panax ginseng* Meyer) (Mathiyalagan et al., 2013). *P. ginseng* is traditionally used as a medicinal herb in oriental medicine in Korea, China, and Japan. Ginsenosides can be classified broadly as protopanaxadiols (PPD) or protopanaxatriols (PPT), and more specifically into major and minor ginsenosides based on the steroidal sapogenin and number of sugar chains and linkages, all of which account for the diverse bioactivities of this class of compounds. Ginsenosides exhibit a vast array of pharmacological efficacies such as anti-tumor and anti-inflammatory effects, as well as protective effects against Alzheimer's disease and anti-diabetic activity (Choi, 2008; Sathishkumar et al., 2012). In recent years, ginsenoside compound K (also referred as 20-*O*-β-(D-glucopyranosyl)-20(S)-protopanaxadiol or CK or IH901 or compound M1) has gained special attention owing to its unique biological properties (Hasegawa, Sung, Matsumiya, & Uchiyama, 1996). CK is one of the primary metabolites obtained after oral administration of various PPD-type ginsenosides by intestinal enzymes. CK has various pharmacological properties including inhibition of proliferation and induction of apoptosis in human colorectal cancer cells and also human hepatoblastoma HepG2 cells (Oh & Lee, 2004; Zhang et al., 2013). In addition, CK inhibits proinflammatory cytokines in lipopolysaccharide (LPS)-stimulated murine peritoneal macrophages (Joh, Lee, Jung, & Kim, 2011).

Although good efficacies of CK have been reported, target specific delivery into tumor sites coupled with solubility issues remains major drawbacks for use of ginsenosides in clinical trials. We recently reported a preparation of poly (ethylene glycol) conjugated CK with improved aqueous solubility compared with free CK (Mathiyalagan et al., 2014). However, the biological applications of such conjugates are not fully understood. In the present study, we aimed to synthesize GC with CK (GC–CK conjugates), which are expected to increase solubility as well as exert the anti-tumor activity of CK. In this conjugate, GC was chosen as hydrophilic polymer that could protect the active agents from proteolytic digestion and provide long circulation characteristics in the blood stream. The physiochemical characteristics of GC–CK conjugates were determined using ^{1}H NMR, Fourier transform infrared spectroscopy (FT-IR), and field emission transmission electron microscopy (FE-TEM) and particle size analyzer. In addition, stability and *in vitro* release behavior of CK from GC–CK conjugates was measured under two different pH-conditions (pH 7.4 and pH 5.0). Lastly, *in vitro* cytotoxicity of GC–CK was evaluated in HT29 (human colon adenocarcinoma), HepG2 (human liver carcinoma), HT22 (mouse hippocampal) and RAW264.7 (murine macrophage) cell lines.

2. Materials and methods

2.1. Materials

GC ($Mw = 4.3 \times 10^5$, degree of deacetylation = 75.2%), N-hydroxyl succinimide (NHS), succinic anhydride, and 1-ethyl-3-(3-dimethylaminopropyl)-carbodiimide·hydrochloride (EDC·HCl) was purchased from Sigma–Aldrich Co. (St. Louis, MO, USA). CK was purchased from Ginseng Genetic Resource Bank (Kyung Hee University, Yongin, South Korea). All other chemicals were of analytical grade and used as received.

2.2. Synthesis of GC–CK conjugates

The synthesis of GC–CK was achieved *via* a two-step process, as shown in Fig. 1. First, carboxylated CK (CK-COOH) was prepared and conjugated to the backbone of GC through amide bond formation. CK-COOH was prepared in the presence of succinic anhydride by using previously reported procedure with slight modification (Yu et al., 2008). Briefly, CK (0.01 g, 0.016 mmol) was dissolved in 2 mL of pyridine/dichloromethane (1:1), to which succinic anhydride (0.0048 g, 0.048 mmol) was added and reacted for 24 h at room temperature. Then, the solvent was evaporated, precipitated in water, filtered, washed, and dried under vacuum to obtain a white powder of CK-COOH. In the second step, GC (0.1 g, 0.53 mmol) was dissolved in 8 mL of distilled water and diluted with 24 mL of methanol, after which CK-COOH (0.038 g, 0.053 mmol), EDC (0.04 g, 0.21 mmol), and NHS (0.024 g, 0.21 mmol) were added and stirred for 24 h at room temperature. The resulting mixture was transferred to a dialysis membrane (MWCO: 14,000) and dialyzed against an excess amount of methanol/distilled water (75:25, v/v) for 1 day, and distilled water for 2 days. Thereafter, the dialyzed solution was freeze-dried to obtain the GC–CK conjugates.

2.3. Characterizations of conjugates

The structures of GC–CK conjugates and their intermediates were confirmed by ^{1}H NMR and FT-IR. ^{1}H NMR spectra were recorded at 300 MHz (JEOL, Tokyo, Japan), for which the samples were dissolved in D_2O or CD_3OD. FT-IR spectra of the conjugates were recorded by a Perkin-Elmer FT-IR spectrophotometer using KBr pellets. The morphology of conjugates was observed using FE-TEM (JEM-2000F, JEOL) operated at an acceleration voltage of 200 kV. To prepare TEM samples, one drop of sample solution was placed onto a 200-mesh copper grid coated with carbon and allowed to air dry. A drop of phosphotunstic acid solution was used for negative staining. The size distribution and stability of conjugates was determined by particle analyzer, for which samples were dispersed in either phosphate-buffered saline (PBS, pH 7.4) or acetate buffer (pH 5.0).

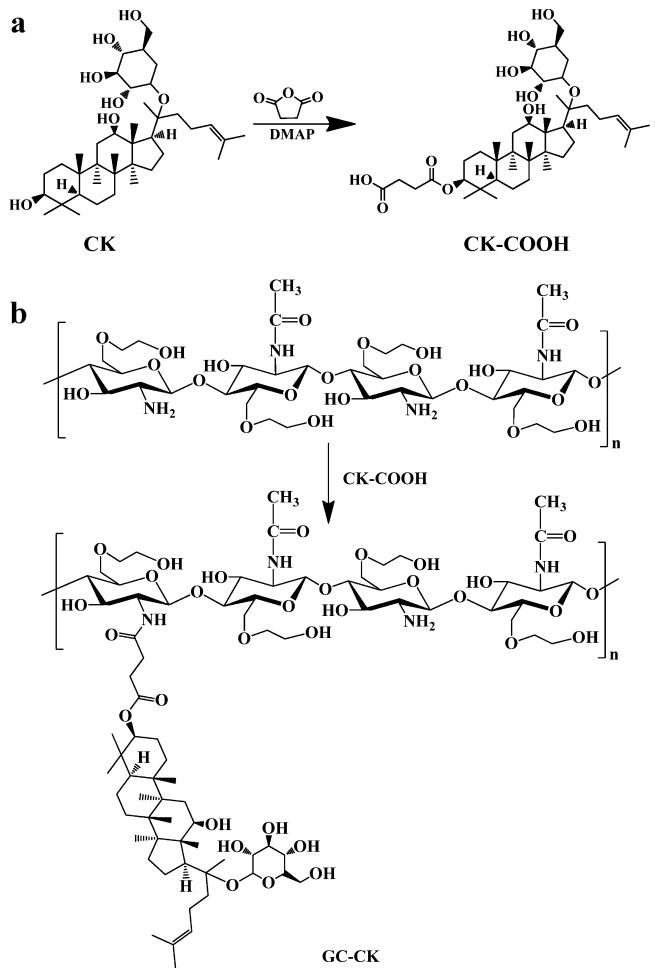

Fig. 1. Synthetic route for preparation of GC–CK conjugates.

2.4. In vitro pH-dependent release of CK from GC–CK conjugates

GC–CK conjugates (3 mg/mL) were dispersed in 1 mL of distilled water and transferred to a cellulose membrane tubes (MWCO: 14,000). The dialysis membrane was then placed in either 30 mL of PBS (pH 7.4) or acetate buffer (pH 5.0), and samples were gently shaken at 37 °C at 120 rpm. At predetermined time intervals, 5 mL samples were withdrawn and replaced with fresh medium. To observe the amount of hydrolyzed CK, the solution was extracted three times with water-saturated *n*-BuOH and evaporated. Then, the amount of CK present in the samples were monitored by HPLC [Agilent, C18 column (3.0 × 50 mm, particle size 2.7 μm)] with acetonitrile (solvent A) and distilled water (solvent B) as mobile phases at 81% B and 19% A for 0 min, 81% B and 19% A for 7 min, 71% B and 29% A for 11 min, 71% B and 29% A for 14 min, 60% B and 40% A for 25 min, 44% B and 56% A for 28 min, 30% B and 70% A for 30 min, 10% B and 90% A for 31.5 min, 10% B and 90% A for 34 min, 81% B and 19% A for 34.5 min, 81% B and 19% A for 40 min, all at a flow rate of 1.0 mL/min. The injection volume of each sample was 5 μL. UV detection was performed at 203 nm.

2.5. In vitro cytotoxicity

The HT-29 (human colon cancer) cell line was purchased from the Korean Cell Line Bank (Seoul, Korea) and cultured in RPMI 1640 medium (Welgene, Inc., Daegu, South Korea) containing 10% (v/v) fetal bovine serum (Welgene, Inc.) and 1% (w/v) penicillin–streptomycin (Welgene, Inc.) in an atmosphere of 5% CO_2 and 95% air at 37 °C. HT-29 cells were seeded separately at a density of 2×10^4 cells/well in 96-well flat-bottomed plates (SPL Life Sciences, Korea). After growing for 24 h, the culture medium was replaced with 100 μL of various concentrations of GC, free CK, or GC–CK and incubated for 24 h at 37 °C. Next, 10 μL of 3-(4, 5-dimethylthiazol-2-yl)-2, 5-diphenyl-tertazolium bromide) (MTT) was added and the plates were incubated for an additional 3 h at 37 °C. The culture medium was then discarded and blue formazan crystals were dissolved with 100 μL of DMSO. The optical density was measured at 570 nm using a Synergy HT multidetection microplate reader (Molecular Devices, BioTek Instruments, Winooski, VT, USA). Similarly, the HepG2 (Li et al., 2013) and HT22 (Li et al., 2012) cell lines were cultured as described and used for MTT assays. In addition, cytotoxicity and LPS (lipopolysaccharide) induced NO (nitric oxide) assays were conducted in RAW264.7 (murine macrophage) cells, as previously described (Lee et al., 2013).

2.6. Statistical analysis

The statistical significance of differences between control *vs* CK and GC–CK groups was determined using a Student's *t*-test. $P < 0.05$ was considered to be significant, and indicated in figures with asterisks (*).

3. Results and discussion

In order to increase the solubility and tumor-targeting of hydrophobic ginsenoside CK, we covalently conjugated it with hydrophilic water-soluble GC through ester bonds, which are hydrolyzed under acidic conditions to release CK for therapeutic purposes. The synthetic procedure used for the preparation of GC–CK conjugates is shown in Fig. 1. First, the CK-COOH was prepared by succinic anhydride treatment, after which CK-COOH was covalently coupled to the amino group of glycol chitosan in the presence of EDC and NHS. The key idea and its working principle of GC–CK conjugates were schematically illustrated in Fig. 2.

3.1. Synthesis and physicochemical characterization of GC–CK conjugates

In order to prepare GC–CK conjugates, we first synthesized carboxylated CK, by reacting CK with succinic anhydride. The obtained CK-COOH was chemically conjugated to the backbone of GC in the presence of EDC and NHS. It has been reported that chemically modified GC conjugates exhibited improved tumor-targeting ability in cell culture system and tumor-bearing mice models. Also, the hydrophilic GC shell provides *in vivo* longevity and targetability to the tumors (Lee, Koo, et al., 2011).

Fig. 3 shows the ^{1}H NMR of GC–CK conjugates, which exhibited the characteristics peak of GC and CK. In the present study, the degree of substitution (DS), defined as the number of CK's in 100 repeating sugar units was calculated based on the integration ratio of the proton peak appearing from the methyl group of CK at 0.68 ppm to that of the N-acetyl peak of GC at 2 ppm. In this study, two GC–CK conjugates were prepared by varying the feed molar ratio of CK to GC. As expected, DS increased as the feed ratio increased (*i.e.* for 0.1 and 0.2 molar ratio of CK, we obtained the conjugates with a DS of 4 and 9, respectively). The GC–CK conjugates synthesized in the study were coded dependent on the DS value. For example, GC–CK4 indicates a conjugates in which the DS of the CK is 4.

Fig. 4a shows the FT-IR spectrum of GC, which included characteristics peaks at 3441 cm^{-1} (O—H stretch overlapped with N—H stretch), 2880 cm^{-1} (aliphatic C—H stretch), 1659 cm^{-1} (amide 1 band, C=O stretch of acetyl group), 1470–1382 cm^{-1} (C—H bend),

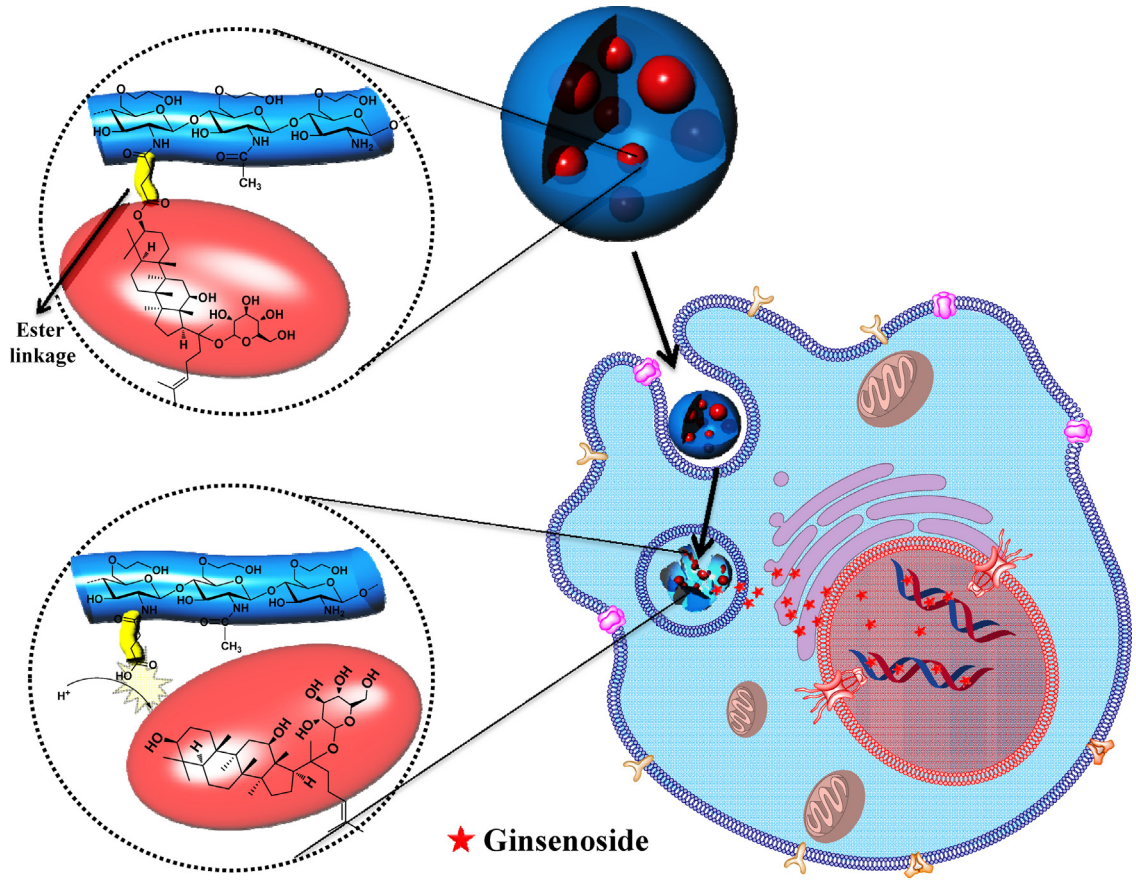

Fig. 2. Graphical illustration of CK release from GC–CK conjugate at the intracellular environment.

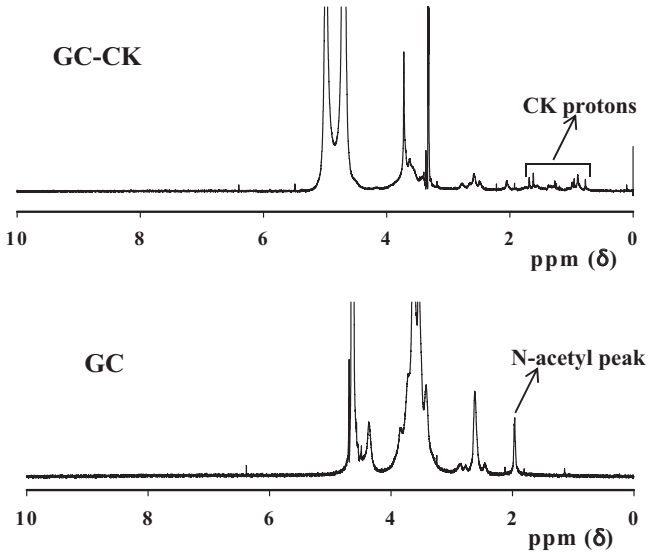

Fig. 3. ^{1}H NMR spectra of the GC–CK conjugate and its intermediates.

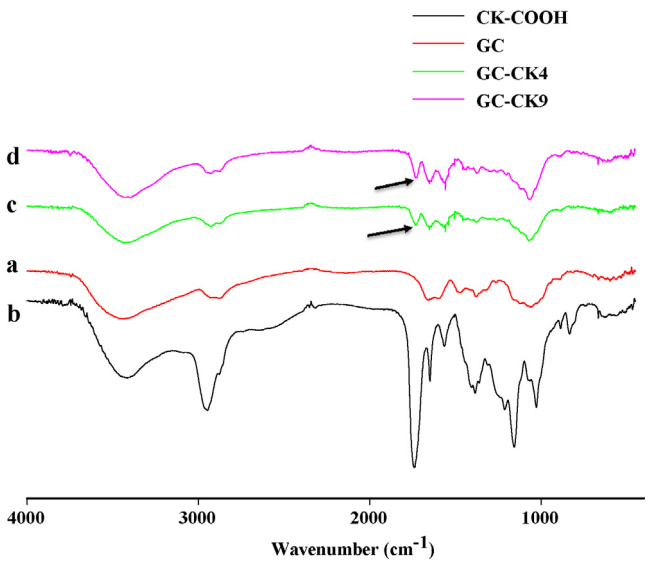

Fig. 4. FT-IR spectra of (a) GC, (b) CK-COOH, (c) GC–CK4, and (d) GC–CK9.

and 1066 cm^{-1} (skeletal vibrations involving the C—O stretch) (Quiñones et al., 2012; Yu et al., 2008). The FT-IR spectra of CK-COOH revealed the presence of a very intense carboxylic C=O bond at 1740 cm^{-1}, which confirmed esterification of CK (Fig. 4b). Compared with GC, the increased intensity of the peak at 1733 cm^{-1} in GC–CK conjugates (Fig. 4c and d) indicated the presence of carbonyl bond (C=O). In addition, the increase in peak intensity at 1558 cm^{-1} (amide II band, N—H bending) and 1653 cm^{-1} (amide I band) confirmed the formation of amide bonds between CK—COOH and GC.

3.2. Size and morphology of GC–CK conjugates

Owing to the amphiphilic nature of GC–CK drug conjugates, they could form self-assembled nanoparticles in an aqueous environment. Thus, a GC hydrophilic shell could cover a hydrophobic

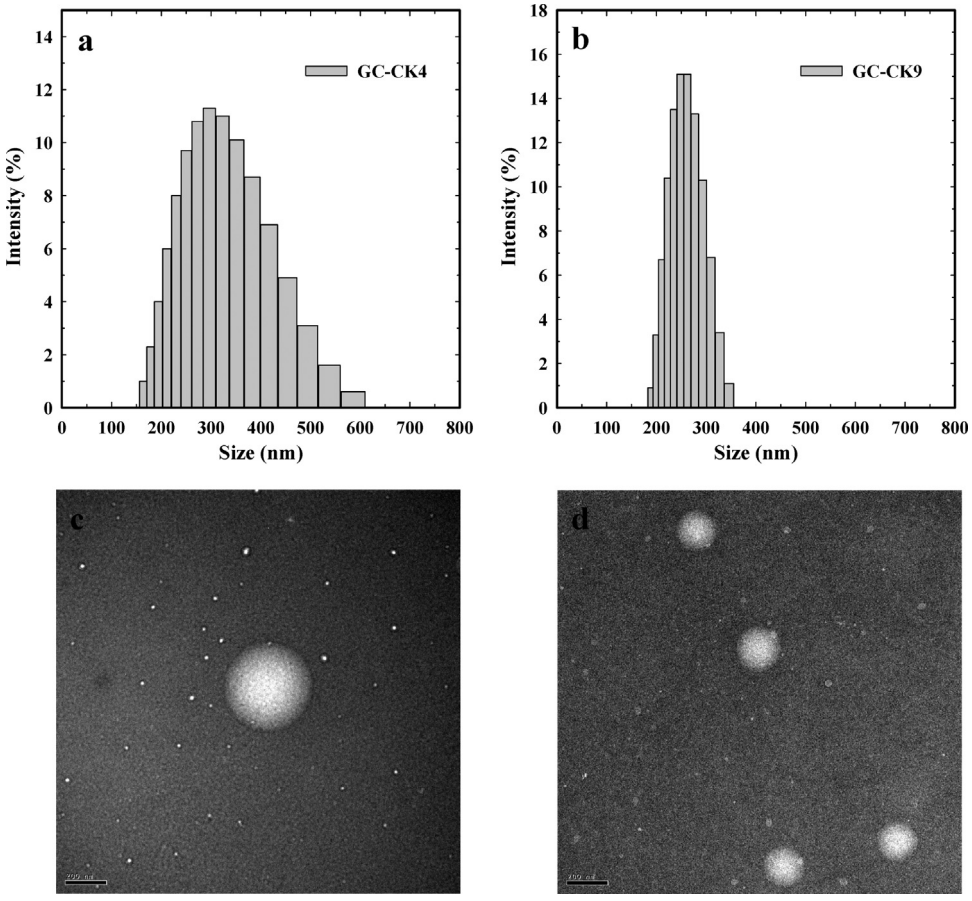

Fig. 5. Particle size of GC–CK conjugates: (a) GC–CK4, (b) GC–CK9. The spherical shaped GC–CK conjugates observed in TEM images: (c) GC–CK4, and (d) GC–CK9. The scale bar represent 200 nm.

CK core and protect it from proteolytic digestion to allow for prolonged circulation in the blood stream. The average diameters of GC–CK4 and GC–CK9 conjugates in aqueous media were 296 nm and 255 nm, respectively (Fig. 5a and b). The size of the nanoparticles decreased as the amount of hydrophobic CK increased, which was attributed to stronger hydrophobic interactions (Yu et al., 2008). Importantly, similar sized GC conjugates were reported to improve tumor-targeting (Lee, Koo, et al., 2011; Min et al., 2008).

Next, the morphology of the conjugates was studied using FE-TEM, which showed that conjugates formed spherical shape particles in aqueous media due to the outer hydrophilic GC and inner hydrophobic CK (Fig. 5c and d). The determined size of the conjugates varied between FE–TEM and particle size analyzer due to a difference in the sample preparation process. The size illustrated by FE–TEM was based on dried state of samples, whereas a particle size analyzer was used to evaluate hydrated samples (Yu et al., 2008). For further studies including stability, *in vitro* CK release, and cytotoxicity, the GC–CK4 was used as a representative conjugates.

3.3. Stability of GC–CK conjugates

Various features such as molecular weight, particles size, blood circulation time, and stability are all important factors that contribute to nanoparticles accumulation at tumor-sites (Cho et al., 2007). Thus, the stabilities of the prepared conjugates were investigated by measuring the particle size at 37 °C in PBS (pH 7.4) as function of time (Fig. 6). The stability of GC–CK4 conjugates was maintained for 8 days, indicating its thermodynamic stability in aqueous media. On the other hand, nanoparticle size was increased

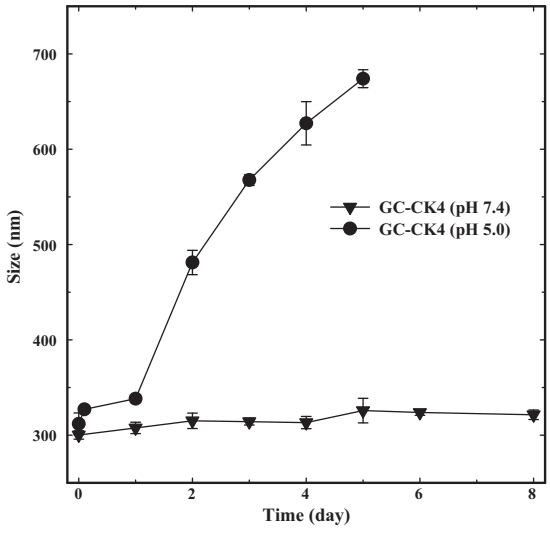

Fig. 6. Stability of GC–CK conjugates in different pH buffers. The error bar represent standard deviation ($n = 3$).

in acidic conditions (pH 5.0), primarily due to the hydrolysis of CK from conjugates, resulting in the formation of large aggregates between the hydrolyzed CK through hydrophobic interaction. The most significant finding from our stability analyses was the high stability of nanoparticles in physiological buffer, which indicated the nanoparticles may exhibit prolonged circulation *in vivo*. From these observations, it was expected that the prepared GC–CK

conjugates stable during the blood circulation, whereas the conjugate triggers the CK release after reaching the tumor site at tumoral acidic pH condition which can be effective for cancer therapy. Specifically, prolonged circulation of higher molecular weight conjugates in the blood consequently enhances tumor targeting by the EPR effect and by minimizing macrophage uptake (Park et al., 2007).

3.4. *In vitro* pH-dependent release of CK from GC–CK conjugates

Polymer conjugated macromolecular prodrugs have the ability to reach tumors due to their leaky vasculature. Further, target drugs are expected to be released at the tumor site following exposure to intracellular stimuli. In particular, pH-responsive drug conjugates have garnered increased attention due to the difference in pH between normal tissues and tumor tissues. Specifically, the intracellular pH of tumor cells (pH 5.0–6.5) is usually much lower than physiological pH conditions (pH 7.4), which has encouraged researchers to develop pH-responsive prodrug formulations to improve therapeutic efficacy. CK release behavior from GC–CK conjugates was monitored by incubating samples at pH 7.4 (physiological) and pH 5.0 (pathophysiological conditions) as a function of time. The percentage of CK release was enhanced under pH 5.0 compared with pH 7.4 as determined by HPLC (Fig. 7). Because the GC–CK conjugate was synthesized *via* an acid-labile ester linkage, the hydrolysis that occurred in the slightly acidic buffer was similar to what would be expected in extracellular solid tumor

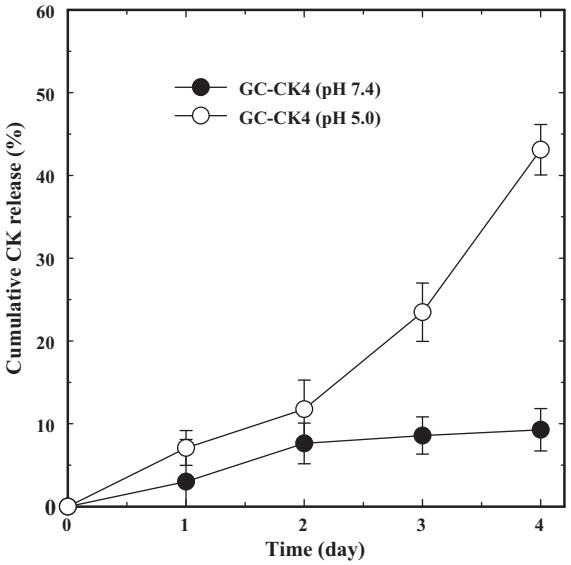

Fig. 7. *In vitro* pH-dependent release of CK from GC–CK conjugates at different pH values. The error bar represent standard deviation ($n = 3$).

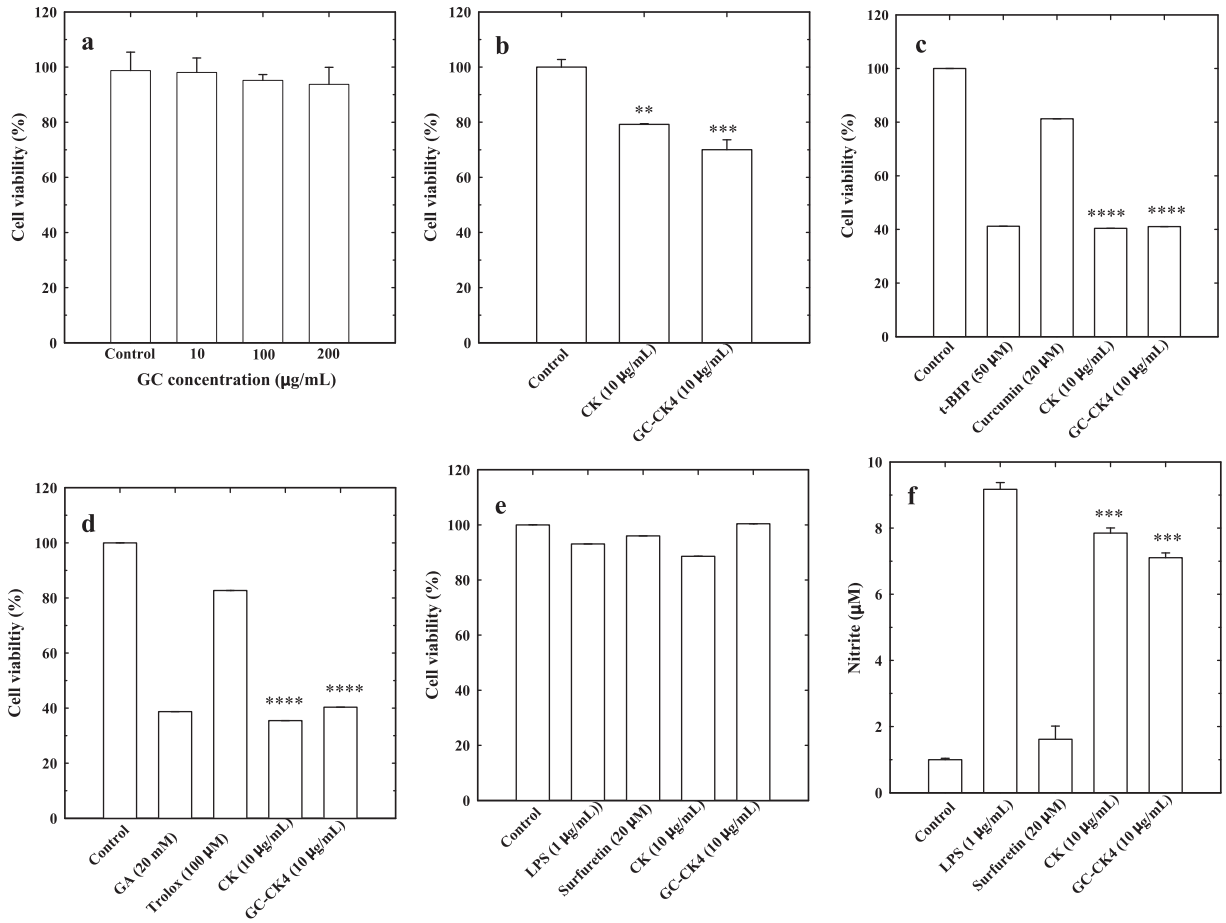

Fig. 8. *In vitro* cytotoxicity of (a) GC and GC–CK conjugates on various cell cancer and inflammatory disease cell lines, (b) HT29 (human colon adenocarcinoma), (c) HepG2 (human liver carcinoma), and (d) HT22 (mouse hippocampal) cell lines. Error bars represent the standard deviation ($n = 3$). ****$P < 0.0001$, ***$P < 0.001$, **$P < 0.01$ *versus* control (untreated group). Curcumin (20 μM) in HepG2, and Trolox (100 μM) in HT22 were used as a positive control, *t*-BHP and GA were used as control. (e) Cell cytotoxicity and (f) inhibition of LPS induced NO production in RAW264.7 (murine macrophage) cells. Error bars represent the standard deviation ($n = 3$). ***$P < 0.001$ compared to the group treated with LPS alone. Surfuretin (20 μM) was used as a positive control. *t*-BHP, tert-butyl hydroperoxide; GA, glutamate; LPS, lipopolysaccharide; NO, nitric oxide.

tissues and intracellular endosomes and lysosomes. Indeed, pH-selective release patterns of various anticancer drugs have been reported (Park et al., 2006; Thambi, Deepagan, et al., 2011; Thambi, Yoon, et al., 2011). Therefore, pH-selective release by ester linkages present in the conjugates may be effective for targeted delivery of CK to pathophysiological sites such as tumors.

3.5. *In vitro* cytotoxicity of the GC–CK conjugates

To observe the *in vitro* anticancer activity of GC–CK conjugate, we examined the cytotoxicity of GC–CK and pure GC in cancer cells by MTT assay. As shown in Fig. 8a, most of the cells were viable and did not exhibit any significant cytotoxic effects at 10, 100 and 200 μg/mL of GC, which supports the biocompatibility of the hydrophilic polymer. GC–CK exhibited significantly higher or similar cytotoxicity compared with CK in HT29 (Fig. 8b) and HepG2 cells (Fig. 8c). However, the GC–CK conjugates exhibited slightly lower toxicity than CK on HT22 cells (Fig. 8d), which was similar to that of other GC conjugates (Duhem et al., 2012; Park et al., 2006; Quiñones et al., 2013). Thus, lower *in vitro* cell cytotoxicity and enhanced *in vivo* antitumor activity of various GC conjugates has been reported previously (Lee, Min, et al., 2011; Min et al., 2008). Further, GC–CK exhibited lower cytotoxicity compared with CK (Fig. 8e) and also inhibited LPS induced NO production in RAW264.7 (murine macrophage) cells to a higher degree than CK (Fig. 8f). Therefore, the GC–CK conjugate described in this study may be a potential candidate to deliver CK to cells in a targeted manner in order to treat cancer and inflammatory diseases.

Development of polymer-drug conjugate with improved tumor-targetability and reduced off-target cytotoxicity is a critical challenge in drug delivery. The chemical conjugation of hydrophilic polymers to poorly insoluble drugs significantly improved their *in vivo* bioavailability and is considered a promising approach. In this regard, the GC–CK conjugates prepared in this exhibited high anticancer in HT29 and HepG2 cells. As expected, the hydrophilic GC did not exhibit cytotoxicity, which implied the biocompatibility of the polymer. From these observations, it was found that the chemical conjugation approach can be used to other ginsenosides to improve their *in vivo* anti-tumor activity.

4. Conclusion

We developed GC–CK conjugates by covalent conjugation of hydrophobic CK to the backbone hydrophilic GC to improve solubility and anti-tumor activity of ginsenoside CK. The conjugates could form self-assembled nanoparticles in physiological buffer (pH 7.4), and exhibited high stability in that condition. However, the conjugates were highly unstable at the mildly acidic pH condition (pH 5.0), similar to that tumor tissues and inflammatory sites. Based on *in vitro* tests, release of CK was significantly enhanced under acidic pH conditions compared with that of normal physiological conditions. Importantly, the GC–CK conjugates exhibited high cytotoxicity in various cell lines. Taken together, these results suggest that GC–CK conjugates may be potentially useful as vehicles for intracellular release of CK. This is the first report of glycol chitosan nanoparticle based approach for delivery of CK, and this approach can be extended to modify other poorly soluble ginsenosides or drug to improve their solubility and tumor-targetability.

Acknowledgements

This research was fully supported by the Korea Institute of Planning & Evaluation for Technology in Food, Agriculture, Forestry & Fisheries (KIPET NO: 309019-3) and a grant from the Next-Generation BioGreen 21 Program (SSAC, grant#: PJ00952903), Rural Development Administration, Republic of Korea.

References

Cho, Y. W., Park, S. A., Han, T. H., Son, D. H., Park, J. S., Oh, S. J., et al. (2007). In vivo tumor targeting and radionuclide imaging with self-assembled nanoparticles: Mechanisms, key factors, and their implications. *Biomaterials*, *28*(6), 1236–1247.

Choi, K. T. (2008). Botanical characteristics, pharmacological effects and medicinal components of Korean *Panax ginseng* C A Meyer. *Acta Pharmacologica Sinica*, *29*(9), 1109–1118.

Deepagan, V. G., Thambi, T., Ko, H., Kang, Y. M., & Park, J. H. (2013). Amphiphilic polysialic acid derivatives: synthesis, characterization, and in-vitro cytotoxicity. *Journal of Nanoscience and Nanotechnology*, *13*(11), 7312–7318.

Duhem, N., Rolland, J., Riva, R., Guillet, P., Schumers, J. M., Jerome, C., Gohy, J. F., & Preat, V. (2012). Tocol modified glycol chitosan for the oral delivery of poorly soluble drugs. *International Journal of Pharmaceutics*, *423*(2), 452–460.

Felt, O., Buri, P., & Gurny, R. (1998). Chitosan: A unique polysaccharide for drug delivery. *Drug Development and Industrial Pharmacy*, *24*(11), 979–993.

Goodarzi, N., Varshochian, R., Kamalinia, G., Atyabi, F., & Dinarvand, R. (2013). A review of polysaccharide cytotoxic drug conjugates for cancer therapy. *Carbohydrate Polymers*, *92*(2), 1280–1293.

Gorczyca, G., Tylingo, R., Szweda, P., Augustin, E., Sadowska, M., & Milewski, S. (2014). Preparation and characterization of genipin cross-linked porous chitosan–collagen–gelatin scaffolds using chitosan–CO_2 solution. *Carbohydrate Polymers*, *102*(0), 901–911.

Hasegawa, H., Sung, J. H., Matsumiya, S., & Uchiyama, M. (1996). Main ginseng saponin metabolites formed by intestinal bacteria. *Planta Medica*, *62*(5), 453–457.

Jayakumar, R., Menon, D., Manzoor, K., Nair, S. V., & Tamura, H. (2010). Biomedical applications of chitin and chitosan based nanomaterials – A short review. *Carbohydrate Polymers*, *82*(2), 227–232.

Joh, E. H., Lee, I. A., Jung, I. H., & Kim, D. H. (2011). Ginsenoside Rb1 and its metabolite compound K inhibit IRAK-1 activation – The key step of inflammation. *Biochemical Pharmacology*, *82*(3), 278–286.

Lee, D. S., Keo, S., Ko, W., Kim, K. S., Ivanova, E., Yim, J., et al. (2013). Secondary metabolites isolated from *Castilleja rubra* exert anti-inflammatory effects through NF-κB inactivation on lipopolysaccharide-induced RAW264.7 macrophages. *Archives of Pharmacal Research*, 1–8.

Lee, S. J., Koo, H., Jeong, H., Huh, M. S., Choi, Y., Jeong, S. Y., et al. (2011). Comparative study of photosensitizer loaded and conjugated glycol chitosan nanoparticles for cancer therapy. *Journal of Controlled Release*, *152*(1), 21–29.

Lee, S. J., Koo, H., Lee, D. E., Min, S., Lee, S., Chen, X., et al. (2011). Tumor-homing photosensitizer-conjugated glycol chitosan nanoparticles for synchronous photodynamic imaging and therapy based on cellular on/off system. *Biomaterials*, *32*(16), 4021–4029.

Li, B., Lee, D. S., Choi, H. G., Kim, K. S., Jeong, G. S., An, R. B., et al. (2012). Involvement of heme oxygenase-1 induction in the cytoprotective and immunomodulatory activities of *Viola patrinii* in murine hippocampal and microglia Cells. *Evidence-Based Complementary and Alternative Medicine*, 128019.

Li, B., Lee, D. S., Kang, Y., Yao, N. Q., An, R. B., & Kim, Y. C. (2013). Protective effect of ganodermanondiol isolated from the Lingzhi mushroom against tert-butyl hydroperoxide-induced hepatotoxicity through Nrf2-mediated antioxidant enzymes. *Food and Chemical Toxicology*, *53*, 317–324.

Maksimenko, A., Alami, M., Zouhiri, F., Brion, J.-D., Pruvost, A., Mougin, J., et al. (2014). Therapeutic modalities of squalenoyl nanocomposites in colon cancer: An ongoing search for improved efficacy. *ACS Nano*, *8*(3), 2018–2032.

Maksimenko, A., Dosio, F., Mougin, J., Ferrero, A., Wack, S., Reddy, L. H., et al. (2014). A unique squalenoylated and nonpegylated doxorubicin nanomedicine with systemic long-circulating properties and anticancer activity. *Proceedings of the National Academy of Sciences*, *111*(2), E217–E226.

Mathiyalagan, R., Subramaniyam, S., Natarajan, S., Kim, Y. J., Sun, M. S., Kim, S. Y., et al. (2013). Insilico profiling of microRNAs in Korean ginseng (*Panax ginseng* Meyer). *Journal of Ginseng Research*, *37*(2), 227–247.

Mathiyalagan, R., Subramaniyam, S., Kim, Y. J., Natarajan, S., Min, J. W., Kim, S. Y., et al. (2014). Synthesis and pharmacokinetic characterization of a pH-sensitive polyethylene glycol ginsenoside CK (PEG–CK) conjugate. *Bioscience, Biotechnology, and Biochemistry*, 1–3.

Min, K. H., Park, K., Kim, Y. S., Bae, S. M., Lee, S., Jo, H. G., et al. (2008). Hydrophobically modified glycol chitosan nanoparticles-encapsulated camptothecin enhance the drug stability and tumor targeting in cancer therapy. *Journal of Controlled Release*, *127*(3), 208–218.

Muzzarelli, C., Tosi, G., Francescangeli, O., & Muzzarelli, R. A. (2003). Alkaline chitosan solutions. *Carbohydrate Polymers*, *338*(21), 2247–2255.

Muzzarelli, R. A. A., Boudrant, J., Meyer, D., Manno, N., DeMarchis, M., & Paoletti, M. G. (2012). Current views on fungal chitin/chitosan, human chitinases, food preservation, glucans, pectins and inulin: A tribute to Henri Braconnot, precursor of the carbohydrate polymers science, on the chitin bicentennial. *Carbohydrate Polymers*, *87*(2), 995–1012.

Nam, H. Y., Kwon, S. M., Chung, H., Lee, S. Y., Kwon, S. H., Jeon, H., et al. (2009). Cellular uptake mechanism and intracellular fate of hydrophobically modified glycol chitosan nanoparticles. *Journal of Controlled Release*, *135*(3), 259–267.

Oh, S. H., & Lee, B. H. (2004). A ginseng saponin metabolite-induced apoptosis in HepG2 cells involves a mitochondria-mediated pathway and its downstream

caspase-8 activation and Bid cleavage. *Toxicology and Applied Pharmacology*, *194*(3), 221–229.

Park, J., Cho, Y., Son, Y., Kim, K., Chung, H., Jeong, S., et al. (2006). Preparation and characterization of self-assembled nanoparticles based on glycol chitosan bearing adriamycin. *Colloid and Polymer Science*, *284*(7), 763–770.

Park, K., Kim, J. H., Nam, Y. S., Lee, S., Nam, H. Y., Kim, K., et al. (2007). Effect of polymer molecular weight on the tumor targeting characteristics of self-assembled glycol chitosan nanoparticles. *Journal of Controlled Release*, *122*(3), 305–314.

Quiñones, J. P., Gothelf, K. V., Kjems, J., Caballero, Á. M. H., Schmidt, C., & Covas, C. P. (2012). Self-assembled nanoparticles of glycol chitosan–ergocalciferol succinate conjugate, for controlled release. *Carbohydrate Polymers*, *88*(4), 1373–1377.

Quiñones, J. P., Gothelf, K. V., Kjems, J., Yang, C., Caballero, A. M. H., Schmidt, C., et al. (2013). Self-assembled nanoparticles of modified-chitosan conjugates for the sustained release of dl-α-tocopherol. *Carbohydrate Polymers*, *92*(1), 856–864.

Sathishkumar, N., Sathiyamoorthy, S., Ramya, M., Yang, D. U., Lee, H. N., & Yang, D. C. (2012). Molecular docking studies of anti-apoptotic BCL-2, BCL-XL, and MCL-1 proteins with ginsenosides from *Panax ginseng*. *Journal of Enzyme Inhibition and Medicinal Chemistry*, *27*(5), 685–692.

Sivasubramanian, M., Thambi, T., & Park, J. H. (2013). Mineralized cyclodextrin nanoparticles for sustained protein delivery. *Carbohydrate Polymers*, *97*(2), 643–649.

Thambi, T., Deepagan, V. G., Ko, H., Lee, D. S., & Park, J. H. (2012). Bioreducible polymersomes for intracellular dual-drug delivery. *Journal of Materials Chemistry*, *22*(41), 22028–22036.

Thambi, T., Deepagan, V. G., Yoo, C. K., & Park, J. H. (2011). Synthesis and physicochemical characterization of amphiphilic block copolymers bearing acid-sensitive orthoester linkage as the drug carrier. *Polymer*, *52*(21), 4753–4759.

Thambi, T., Deepagan, V. G., Yoon, H. Y., Han, H. S., Kim, S.-H., Son, S., et al. (2014). Hypoxia-responsive polymeric nanoparticles for tumor-targeted drug delivery. *Biomaterials*, *35*(5), 1735–1743.

Thambi, T., Yoon, H. Y., Kim, K., Kwon, I. C., Yoo, C. K., & Park, J. H. (2011). Bioreducible block copolymers based on poly (ethylene glycol) and poly (γ-benzyl l-glutamate) for intracellular delivery of camptothecin. *Bioconjugate Chemistry*, *22*(10), 1924–1931.

Yu, J. M., Li, Y. J., Qiu, L. Y., & Jin, Y. (2008). Self-aggregated nanoparticles of cholesterol-modified glycol chitosan conjugate: Preparation, characterization, and preliminary assessment as a new drug delivery carrier. *European Polymer Journal*, *44*(3), 555–565.

Zhang, Z., Du, G. J., Wang, C. Z., Wen, X. D., Calway, T., Li, Z., et al. (2013). Compound K, a ginsenoside metabolite, inhibits colon cancer growth via multiple pathways including p53-p21 interactions. *International Journal of Molecular Sciences*, *14*(2), 2980–2995.